Geomechanics and Engineering, *Vol. 30, No. 6 (2022) 503-515*
https://doi.org/10.12989/gae.2022.30.6.503

Application of rock mass index in the prediction of mine water inrush and grouting quantity

Jinhai Zhao*[1,2], Qi Liu**[1,2], Changbao Jiang***[1,2,4] and Wang Defeng[3]

[1]*State Key Laboratory Breeding Base for Mining Disaster Prevention and Control, Shandong University of Science and Technology, Qingdao 266590, China*
[2]*College of Energy and Mining Engineering, Shandong University of Science and Technology, Qingdao 266590, China*
[3]*Institute of Mining and Special Civil Engineering, Technical University of Bergakademie Freiberg, Freiberg, 09599 Dresden, Germany*
[4]*State Key Laboratory of Coal Mine Disaster Dynamics and Control, School of Resources and Safety Engineering, Chongqing University, Chongqing 400030, China*

(*Received April 23, 2022, Revised July 17, 2022, Accepted August 16, 2022*)

Abstract. The permeability coefficient is an essential parameter for the study of seepage flow in fractured rock mass. This paper discusses the feasibility and application value of using readily available RQD (rock quality index) data to estimate mine water inflow and grouting quantity. Firstly, the influence of different fracture frequencies on permeability in a unit area was explored by combining numerical simulation and experiment, and the relationship between fracture frequencies and pressure and flow velocity at the monitoring point in fractured rock mass was obtained. Then, the stochastic function generation program was used to establish the flow analysis model in fractured rock mass to explore the relationship between flow velocity, pressure and analyze the universal law between fracture frequency and permeability. The concepts of fracture width and connectivity are introduced to modify the permeability calculation formula and grouting formula. Finally, based on the on-site grouting water control example, the rock mass quality index is used to estimate the mine water inflow and the grouting quantity. The results show that it is feasible to estimate the fracture frequency and then calculate the permeability coefficient by RQD. The relationship between fracture frequency and RQD is in accordance with exponential function, and the relationship between structure surface frequency and permeability is also in accordance with exponential function. The calculation results are in good agreement with the field monitoring results, which verifies the rationality of the calculation method. The relationship between the rock mass RQD index and the rock mass permeability established in this paper can be used to invert the mechanical parameters of the rock mass or to judge the permeability and safety of the rock mass by using the mechanical parameters of the rock mass, which is of great significance to the prediction of mine water inflow and the safety evaluation of water inrush disaster management.

Keywords: fracture frequency, grouting estimation, permeability, RQD, water inflow

1. Introduction

The prediction method of mine inflow is mainly qualitative analysis. For example, analytical method and analogy method only consider the local characteristics of the mine. This does not fully reflect the reality of the mine. However, the traditional numerical simulation method regards the stratum as isotropic material, which ignores the actual characteristics of the simulated object. The process of groundwater migration to mining space presents complex forms such as nonlinear flow. Therefore, it is difficult to give a reasonable quantitative analysis model. The difference of prediction results between different prediction methods cannot reflect the actual hydrogeological situation (Annaidh *et al.* 2013 Cheng *et al.* 2020, Wan *et al.* 2018, Du *et al.* 2009, Chen *et al.* 2009, Yang *et al.* 1995). The characteristics of anisotropy and heterogeneity of mine hydrogeology. It is difficult to be explained by simple analytical methods and other theoretical models. The numerical model has flexibility and is a calculation method with high prediction accuracy. However, the accuracy of numerical simulation method is mainly restricted by the rationality of simulation parameters.

The key to predict mine inflow is to obtain numerical simulation parameters such as permeability of rock mass. At present, there are three main methods to measure the permeability of surrounding rock: geometric measurement, water pressure test and mathematical model inversion. However, in most engineering practice, seepage simulation is mainly based on equivalent porous media theory (Zeng *et al.* 2022a, Zhao *et al.* 2022).

This cannot reflect the discrete characteristics of rock mass fractures (Wan *et al.* 2018, Khorasani *et al.* 2019, Euser *et al.* 2019). In recent years, the calculation of rock mass permeability based on statistical methods has been developed, which can more accurately reflect the anisotropy of rock mass permeability (Wu 1998, Morrison *et al.* 2019).

*Corresponding author, Ph.D.
E-mail: Jinhai.zhao@sdust.edu.cn
**Corresponding author, Ph.D.
E-mail: xihuancicuo@163.com
***Corresponding author, Professor
E-mail: jcb@cqu.edu.cn

ISSN: 2005-307X (Print), 2092-6219 (Online)

Deere proposed the concept of rock quality Designation (RQD) based on drilled cores (Deere 1963). It is defined as the percentage of the length of a cylindrical core greater than 10 cm to the current footage. In the application of rock mechanics, RQD is a common index to reflect the integrity of rock mass (Wan *et al.* 2022, Zeng *et al.* 2022b). It has been widely used in engineering rock mass quality evaluation and rock mass property classification (Chen *et al.* 2005, Guo *et al.* 2017, Jha *et al.* 2014, Munoz *et al.* 2016, Cai *et al.* 2022, Zhou *et al.* 2020). Studies on permeability of rock mass show that the relationship between permeability coefficient and RQD satisfies an exponential function (Lin 2010, Karatela *et al.* 2018, Mottahedi *et al.* 2019). The permeability coefficient can be obtained by borehole water pressure test (Zhao *et al.* 2018). However, this kind of test is expensive and difficult to reflect local characteristics. Finally, only generalized model parameters can be obtained. Accurate calculation of permeability coefficient is very important for the accuracy of numerical simulation. How to accurately and conveniently calculate the permeability coefficient of rock mass can guide the field production, which has important practical significance. The number, opening and direction of structural planes (or cracks) in rock mass reflect the integrity of rock mass. At the same time, it has an important influence on the permeability of rock mass. In the study of the correlation between rock mass quality index and rock permeability, domestic and foreign researchers have actively explored. It has obtained more beneficial characteristics and laws. Jiang *et al.* (Jiang *et al.* 2009, Sweetenham *et al.* 2017) explored the relationship between burial depth and permeability. With the increase of depth, the mean value of RQD increases gradually, while the mean value of permeability coefficient decreases and has a good correlation. Liu *et al.* (Liu *et al.* 2007, Wan *et al.* 2018) explored the relationship between fractal dimension of structural plane distribution in rock mass and rock mass quality grade. They put forward a scheme of rock mass quality evaluation based on fractal dimension of rock discontinuities distribution. The relationship between rock mass fracture frequency and rock mass quality index is established. Zhang *et al.* (zhang *et al.* 2005, Ibishi *et al.* 2022, Kim *et al.* 2018) corrected some deficiencies of fractal dimension in evaluating rock quality index RQD. They put forward the quantitative evaluation index of rock mass quality. In this paper, a two-dimensional discrete fracture network generation program is written. Combined with the boundary element method, the secondary development is carried out and the water inflow of roadway is calculated, which provides a feasible calculation method for the prediction of water inflow of mine pit.

Based on the finite element numerical simulation, the discrete fracture network of rock mass permeability is directly reflected by the correlation between rock mass quality index and rock mass permeability. A numerical simulation method for daily water inflow prediction and grouting process prediction is presented. In this paper, fracture frequency is expressed as the number of fractures contained in the rock core per unit drilling length which is generally 2 meters. Firstly, the influence of different orthogonal fracture frequencies on permeability in unit area is monitored. In the process of fracture seepage, the relationship between fracture frequency, pressure and flow rate of monitoring point is explored. Then, the random crack generation program is applied to establish a two-dimensional crack numerical model. The function relation between flow velocity and pressure in fractured rock mass is obtained. Finally, based on the field grouting engineering example, the mine grouting quantity is estimated by using the rock mass quality index. The results show that RQD can estimate the change of permeability coefficient before and after coal mining. The quantitative relationship between RQD, structural frequency and permeability was obtained. Rock mechanics parameters can be used to judge the permeability and safety of rock mass. The research results are great significant to the prediction of mine water inflow, water inrush disaster control and safety evaluation. It should be pointed out that, the calculation method of water inflow in this paper must satisfy that there cannot be centralized seepage channels. The rock mass as a whole is micro-fracture, and the correlation between RQD and water pressure and seepage parameters can only exist in rock mass that can be described by RQD.

In this paper, fracture frequency is expressed as the number of fractures contained in the rock core per unit drilling length which is generally 2 meters.

2. Seepage experiment and simulation analysis of fractured rock mass

2.1 Relationship between fracture frequency and flow velocity

In 1978, the Laboratory of the International Society for Rock Mechanics suggested that 10 parameters (Wei *et al.* 2005, Yamada *et al.* 1968, Komurlu *et al.* 2016, Lawal *et al.* 2022, Li *et al.* 2017), such as discontinuities of discontinuities, discontinuities, surface roughness, relief, filling and fracture group number, should be used to describe the discontinuities of rock masses. These parameters describe the geometrical and structural characteristics of fracture distribution in rock mass (Lv *et al.* 2019, Ghyasvand *et al.* 2022, Mahmoodzadeh *et al.* 2022, Samanta *et al.* 2018). It is important for quantitative analysis of rock mass structure. For the calculation of permeability tensor of underground rock mass, fracture occurrence affects the dominant permeability direction of fractured rock mass. The spacing and width of cracks and filling conditions control the permeability of rock mass, and roughness and relief also have an important influence on the permeability of rock mass (Wei *et al.* 2005, Deere 1963, Zhao *et al.* 2020, Zhao *et al.* 2019, Varun *et al.* 2017). The in-situ drilling results show that there are a large number of primary fractures in rock mass, which affect the strength and dominant permeability direction of rock mass. The cores obtained from field sampling are shown in Fig. 1.

In order to study the quantitative relationship between the number of fractures in rock mass and the permeability of rock mass, orthogonal fracture network models with

Fig. 1 Core fracture distribution diagram

different number of fractures were firstly constructed by numerical simulation (Fig. 2, Fig. 3 and Fig. 4). The seepage law and influencing factors in fracture network model are analyzed. As for the test, rock samples with different vertical fracture frequencies were made (Fig. 3). The seepage experiment of fractured rock mass is carried out on a triaxial seepage coupling experiment machine. The relationship between fracture frequency and permeability was investigated. The main research object is vertical fracture. The fissure openings are 1×10^{-4} m. The model size is 100×100×200 mm. The number of vertical cracks is 1, 3, 7 and 9, respectively. The crack opening is controlled by the thickness of stainless steel gasket. Experimental boundary conditions and samples are shown in Fig. 3. According to the basic assumption of fluid-structure coupling analysis, it is assumed that the rock block is impervious to water, and the seepage in rock mass is only through cracks. The relationship between normal stress and fracture surface deformation and water conductivity is considered. The fluid-structure coupling cross iteration method is used. A numerical model for coupled seepage and stress analysis of orthogonal fractured rock mass is established. Matlab software is used to write crack generation program. Combined with Comsol Multiphysics numerical analysis software, the block stress, seepage and rock fracture distribution analysis modules are integrated together. Numerical analysis models with different fracture frequencies were established to explore the relationship between fracture frequency and permeability. The parameters of model size and crack opening are the same as those of physical experiment. At the same time, the number of transverse fractures was increased to explore the effect of vertical fractures on permeability. Fig. 4 shows the simulation diagram of model water pressure distribution under the influence of different orthogonal fracture frequencies.

It can be seen from the experimental results and

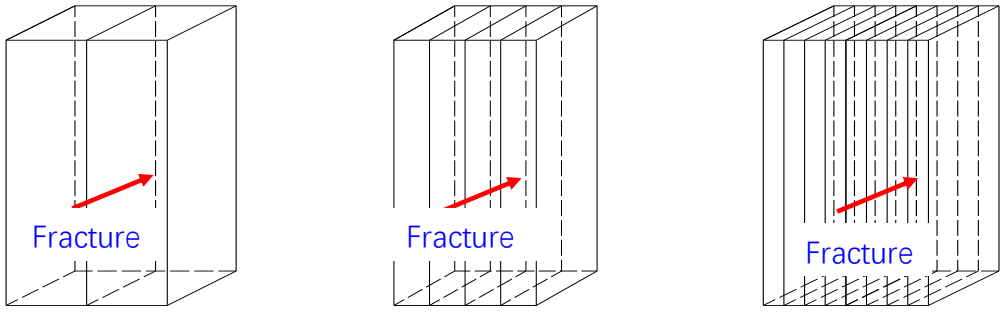

(a) The fracture frequency is 1 (b) The fracture frequency is 3 (c) The fracture frequency is 7

Fig. 2 Schematic diagram of specimens with different crack frequencies

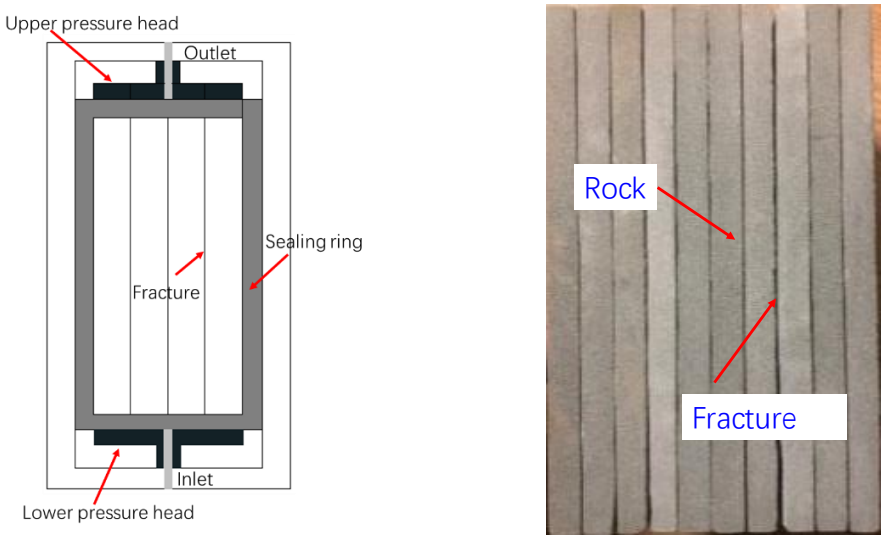

Fig. 3 Experimental boundary conditions and samples

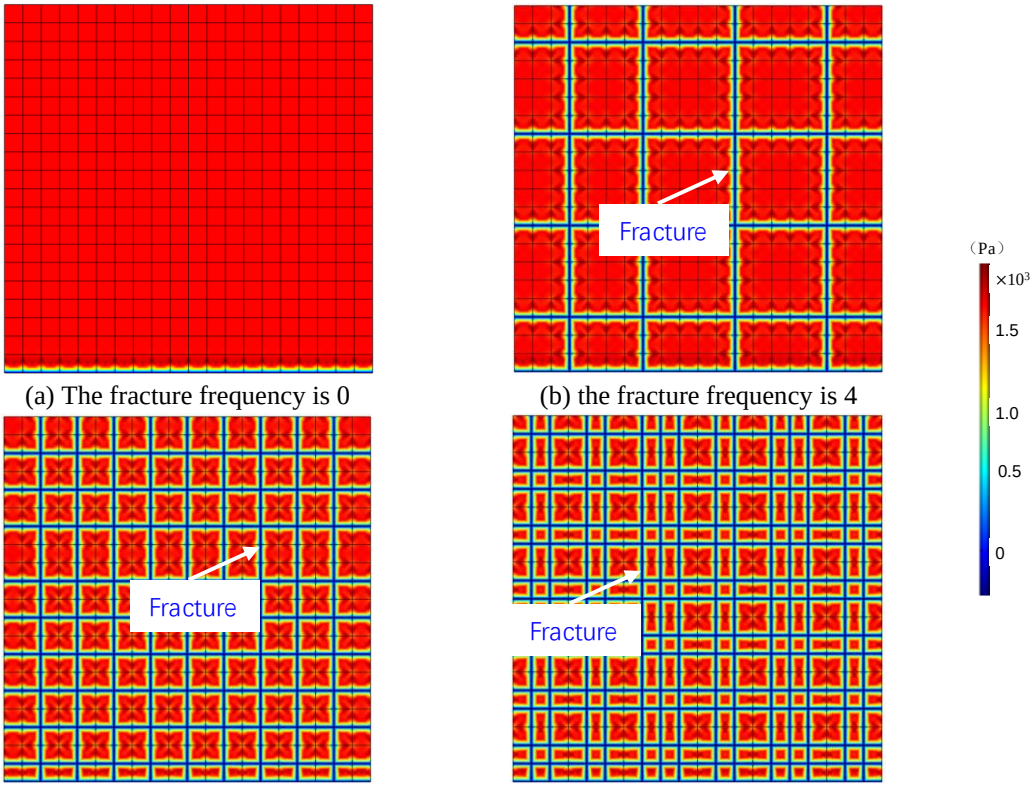

(a) The fracture frequency is 0 (b) the fracture frequency is 4

(c) the fracture frequency is 9 (d) the fracture frequency is 14

Fig. 4 Simulation diagram of water pressure distribution of the model with different crack frequencies

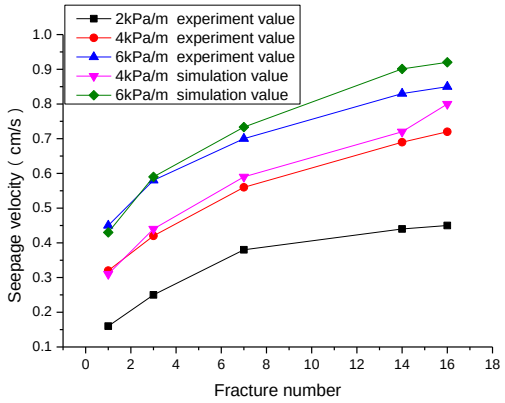

Fig. 5 Experimental results and numerical simulation results of seepage velocity at different fracture frequencies

simulation results of seepage velocity with different fracture frequencies (Fig. 5) that under the same pressure gradient, when the fracture frequency is small and the seepage velocity is low (<3 cm/s in the figure), the flow law of fluid in the fracture network is close to the linear state, that is, approximately follows the linear seepage law. However, as the seepage velocity increases, the seepage curve gradually bends toward the horizontal axis (the fracture frequency axis), presenting obvious nonlinear seepage characteristics (Fig. 5). The numerical simulation results of orthogonal fracture network show that when the number of fractures is the same in the transverse direction (perpendicular to the direction of seepage), the more fractures in the vertical direction (parallel to the direction of seepage), the greater the seepage velocity of the model, and the influence of fracture growth perpendicular to the direction of seepage is little.

With the increase of fracture frequency, the mean value of seepage velocity increases gradually, and the seepage curve curves to the horizontal axis (fracture frequency axis). It also presents obvious nonlinear seepage characteristics. The experimental results show that the relationship between seepage velocity and fracture frequency is an exponential function, which is the same as the result obtained in this paper (Lu *et al.* 2010, Vaziri *et al.* 2022, Xue *et al.* 2020). The results show that the numerical simulation method considering fracture frequency can be used to predict seepage velocity and seepage flow in fractured rock mass.

2.2 Relationship between fracture frequency and seepage flow rate

In nature, fractures in rock mass are distributed randomly and fluid flows mainly in fracture networks. Currently, Monte-Carlo method is recognized as a relatively accurate random statistical method for constructing random fracture network (Cheng *et al.* 2020, Wan *et al.* 2018, Zhou *et al.* 2020). In this paper, monte Carlo method and linear congruence method are used to generate random fracture networks, which establishes the finite element numerical model of random fractured rock mass.

$$\begin{cases} x_{n+1} = (ax_n + c) \times (modM) \\ r_n = \frac{x_n}{m} \\ x_0 \end{cases} \quad (1)$$

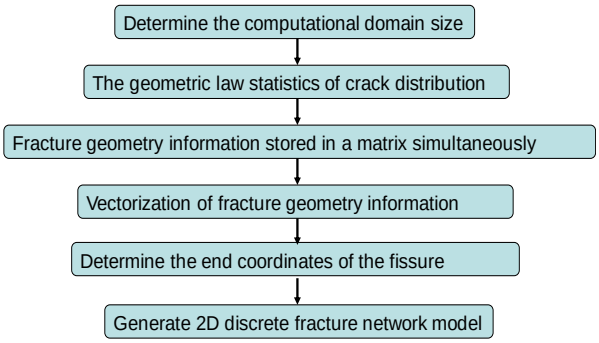

Fig. 6 Generating flow chart of discrete crack network

Where, mod M means mod to modulus. a is the coefficient. c is delta. x_0 is set to the initial value. r_n is a random number within [0,1].

The opening degree of cracks follows lognormal distribution (Cheng *et al.* 2020, Wan *et al.* 2018)

$$F(x) = \int_{-\infty}^{x} f(t)\,dt = \frac{1}{\sigma\sqrt{2\pi}} \int_{-\infty}^{x} e^{\frac{1}{2}\left(\frac{t-t^{-2}}{\sigma}\right)}\,dt \qquad (2)$$

The normal random function generated is:

$$x = \mu_x + \sigma_x \cdot \sqrt{-2\ln(rand)} \cdot \cos(2\pi \cdot rand) \qquad (3)$$

Where, the value of x is a random number that follows normal distribution. rand is a random number distributed by an interval uniform function (Wan *et al.* 2018, Du *et al.* 2009, Priest *et al.* 1967).

Based on the basic theory of Monte-Carlo method, MATLAB software was used to set the types of distribution functions obeyed by each fracture (Wan *et al.* 2018). Random geometrical parameters are generated in rock fracture networks. For example, the location, size and direction of the fractures in the study area. The specific process of computer generated program of discrete fracture network is as follows. First, a global coordinate system is defined and the computational domain size is determined. Second, the number of cracks N in the network model is given. The location and trace length of each fracture are determined by random function. Third, the fractures of all groups are stored in a matrix simultaneously. According to the above steps to determine the end coordinates of all groups of cracks. The random discrete fracture network model in rock mass is generated by executing the drawing command in MATLAB, and the execution process is shown in Fig. 6. In order to ensure the consistency of seepage outlet and the rationality of calculation results, the same fracture length is selected as the flow outlet.

The fitting coefficients of different fracture frequencies and pressures are shown in Table 1. The fitting function formula is

$$P = A_1 \times \exp\left(-\frac{\lambda}{t_1}\right) + P_0 \qquad (4)$$

Where, P is the water pressure. λ is the number of fractures per unit area (fracture frequency for short). P_0, A_1 and t_1 are fitting parameters. See Table 1 for specific values.

The distribution of model water pressure under the influence of different random fracture frequencies is shown in Fig. 8. With the increase of fracture frequency, the

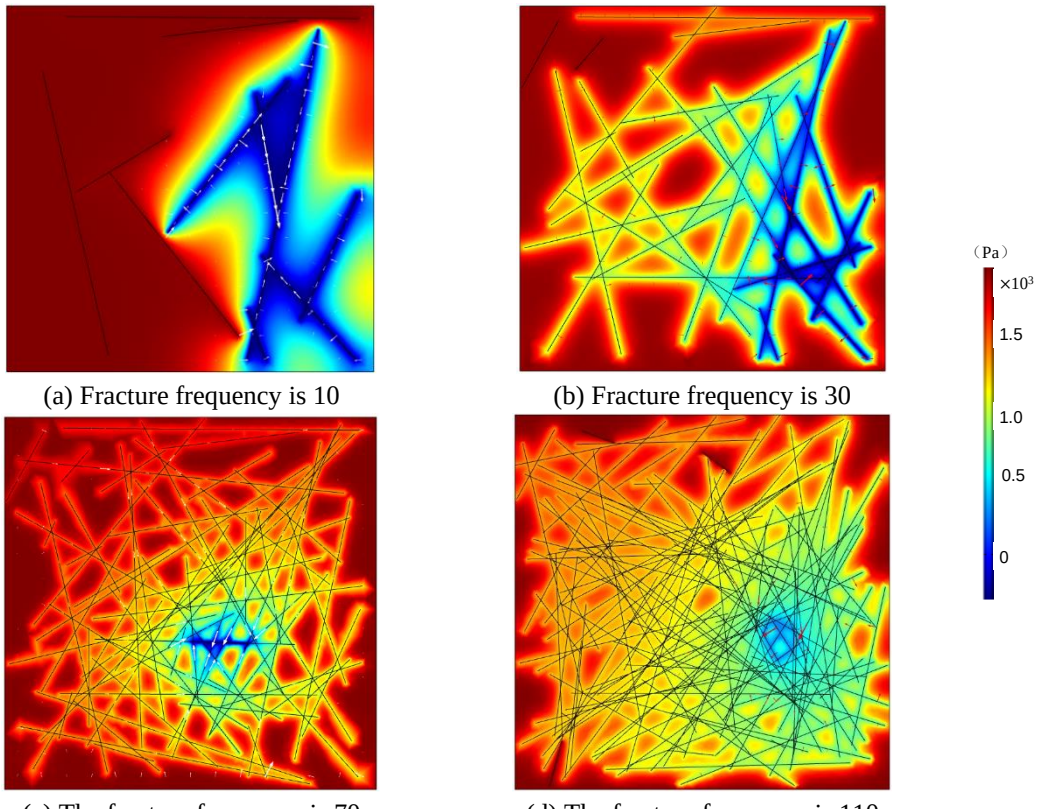

(a) Fracture frequency is 10 (b) Fracture frequency is 30

(c) The fracture frequency is 70 (d) The fracture frequency is 110

Fig. 7 Water pressure distribution with different crack frequencies

Table 1 Fitting coefficient of crack frequency and pressure

Coefficient / Frequency	A_1	t_1	P_0	Degree of fitting
10	4.1	34.7	10733	0.992
30	1.15	28.7	16485	0.996
70	1.38	17.46	14152	0.993
110	1.36	14.92	14637	0.990

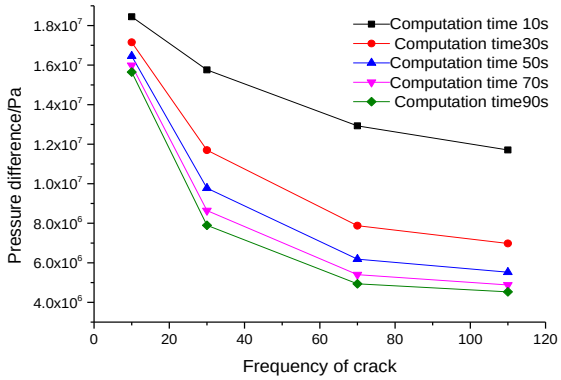

Fig. 8 Relationship between crack frequency and pressure

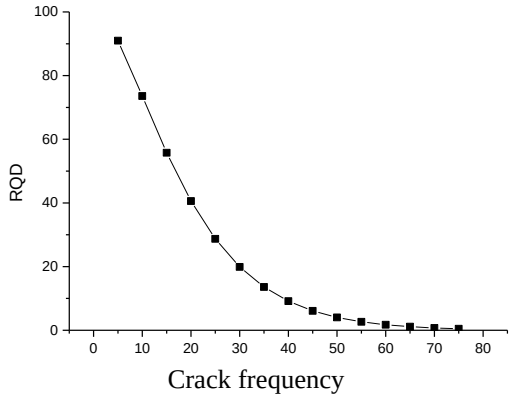

Fig. 9 Relationship between crack frequency and *RQD*

average seepage velocity gradually increases, the seepage curve gradually bends to the fracture frequency axis, and the pore pressure decreases rapidly in an exponential function relationship. This presents nonlinear seepage characteristics (Jiang *et al.* 2009). The variation relationship between fracture frequency and pressure is shown in Formula 4.

2.3 Relationship between RQD and fracture frequency

In general, it is difficult to directly measure the fracture density of rock mass. However, the density (frequency) and the opening value of the fracture can be calculated by the *RQD* value obtained during drilling. The frequency of fractures in rock mass can be obtained according to the relationship between *RQD* and discontinuity frequency established by Priest and Hudson (PRIEST *et al.* 1976, Hudson *et al.* 1997). The relationship between fracture frequency and *RQD* is shown in Formula 5 and Fig. 9

$$RQD = 100(1 + 0.1\lambda)e^{-0.1\lambda} \tag{5}$$

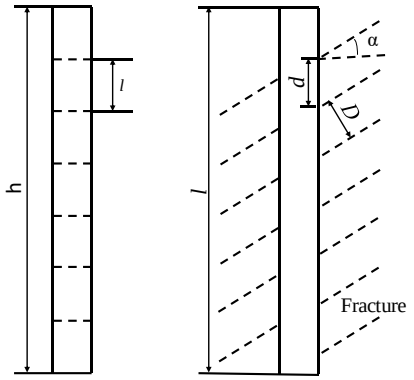

Fig. 10 Relationship between fracture interval and drilling depth

Field statistics show that the lower limit of the average crack opening is 10^{-3} mm, which is similar. Scholars at home and abroad have systematically studied the distribution of crack opening degree. Zhou *et al.* (1998) conducted compression tests of granite with through-through joints. They determined that the mean mechanical opening of the fissure was 75 μm. The study of Berbsky *et al.* proves that the fluid movement in the fracture still conforms to Darcy's linear law when the fracture opening is smaller (<0.25 μm). Therefore, the permeability tensor is calculated by measuring the average gap width value. For tensile joints, the gap width decreases rapidly with increasing depth due to the influence of gravity field, and the opening of shear joints changes little with increasing depth. The gap width can be considered constant. The results show that the rock mass vertical stress is the maximum principal stress at 400-600 m. At this point, tensile joints and shear joints can be approximately regarded as the same gap width (Zhou *et al.* 1998).

In hydraulics, the equivalent hydraulic gap width (e) is generally used to calculate the permeability tensor. The calculation formula is

$$e = \frac{E^2}{JRC^{2.5}} \tag{6}$$

Where, E is the average width of crack. *JRC* is the surface roughness of the crack, ranging from 0 to 20.

Suppose the hole depth is h. The drilling circulating footage length is l. The feed footage of each cycle is unit length and the number of cracks in unit length is λ. The dominant direction of fracture dip Angle is α. The average spacing between cracks per unit length along the direction of drilling is

$$d = \frac{l}{\lambda} \tag{7}$$

The true spacing is

$$D = \frac{l\cos\alpha}{\lambda} \tag{8}$$

In fractured media, the spatial structure of fracture network determines the permeability of the medium. It is generally believed that the superposition of permeability of rock mass can obtain the calculation formula of permeability tensor of fractured rock mass (Zhou *et al.* 2004, Wang *et al.* 2006)

$$K = \sum_{i=1}^{n} K_i = \sum_{i=1}^{n} K_{ei} \cdot a(\beta_i, \gamma_i) \quad (9)$$

Where

$$a(\beta_i, \gamma_i) = \begin{bmatrix} 1-\cos^2\beta_i \sin^2\gamma_i & -\sin\beta_i \cos\beta_i \sin^2\gamma_i & -\cos\beta_i \sin\gamma_i \cos\gamma_i \\ -\sin\beta_i \cos\beta_i \sin^2\gamma_i & 1-\sin^2\beta_i \sin^2\gamma_i & -\sin\beta_i \sin\gamma_i \cos\gamma_i \\ -\cos\beta_i \sin\gamma_i \cos\gamma_i & -\sin\beta_i \sin\gamma_i \cos\gamma_i & 1-\cos^2\gamma_i \end{bmatrix}$$

$$K_{ei} = \frac{ge^3}{12v_w D} \quad (10)$$

Where, K_i represents the permeability tensor of group i fissure. γ_i represents the tendency of group i fissure. γ_i represents the dip Angle of group i fissure. v_w is the kinematic viscosity of the fluid. g is the acceleration of gravity.

Through the eigenvalue and eigenvector of K, the principal value (K_1, K_2, K_3) of the permeability tensor of fractured rock mass and the principal direction of the permeability tensor can be obtained. Generally, the geometric average of the three principal values of the permeability coefficient is taken as the comprehensive permeability coefficient k_0

$$k_0 = \sqrt[3]{K_1 K_2 K_3} \quad (11)$$

3. Estimated water inflow of fractured rock mass

In order to verify the rationality of using RQD parameters to predict mine water inflow, this paper carries out numerical simulation analysis and verification against the background of water inflow change in a mine in Feicheng. The mine working face is 203 m long, 83 m long, mining depth is 144 m, coal seam dip Angle is 10°. The working face is located in a water-rich area with karst fissures. The direct aquifer is xujiazhuang limestone of Benxi Formation, with a thickness of 12.24 m and a water level of +56 m. It is only about 12.5 m away from The Ordovician Limestone and closely related to the ordovician limestone hydraulic power. The Ordovician Limestone aquifer has a thickness of about 800 m and is rich in water. It is the main recharge water source of the Ordovician Limestone. The numerical model established according to geological conditions is shown in Fig. 11. The waterproof layer from coal floor to wuhui (aquifer) is mainly clay rock and siltstone, and the thickness of the waterproof layer is about 16.5 m. The working face is in limestone runoff zone. Under the influence of coal floor damage caused by coal mining, the risk of floor water inrush is high and the probability of floor water inrush is greater than 95%.

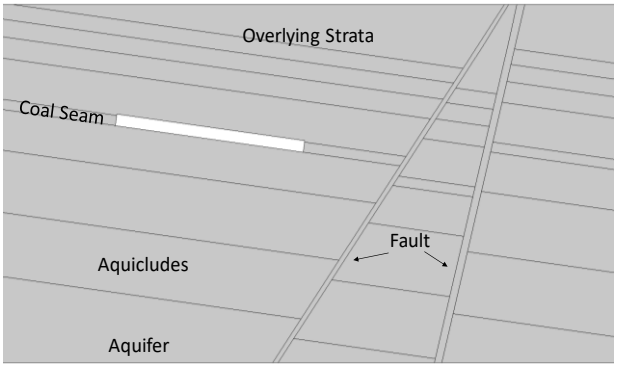

Fig. 11 Calculation model diagram

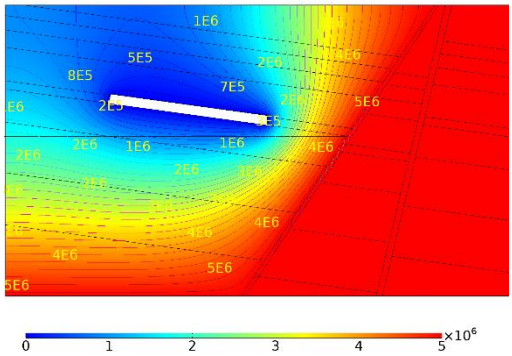

(a) Stope water pressure distribution when RQD value is 80

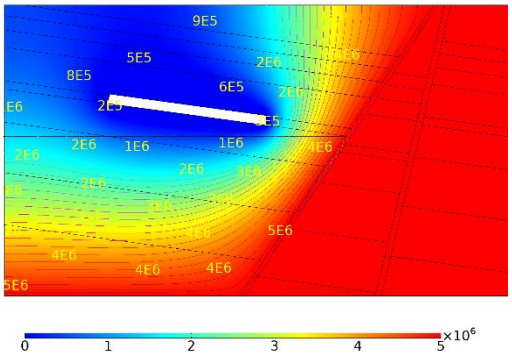

(b) Stope water pressure distribution when RQD value is 60

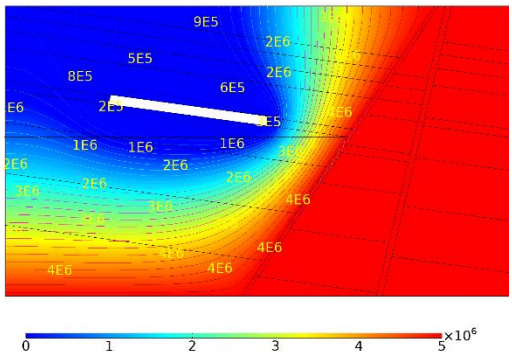

(c) Stope water pressure distribution when RQD value is 30

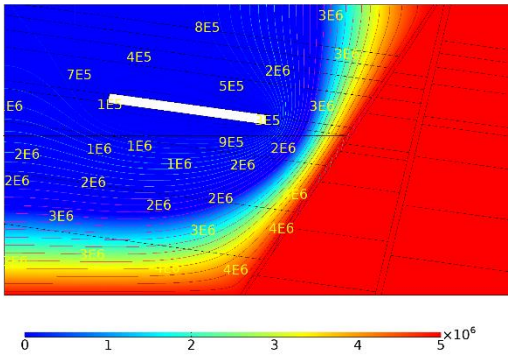

(d) Stope water pressure distribution when RQD value is 10

Fig. 12 Characteristics of pore water pressure distribution in mining floor with different RQD values

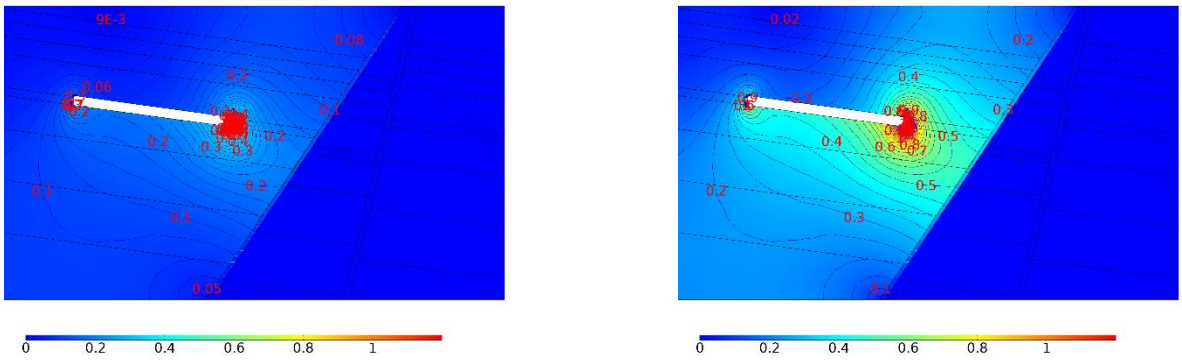

(a) Water seepage velocity distribution when RQD value is 80 (b) Water seepage velocity distribution when RQD value is 60

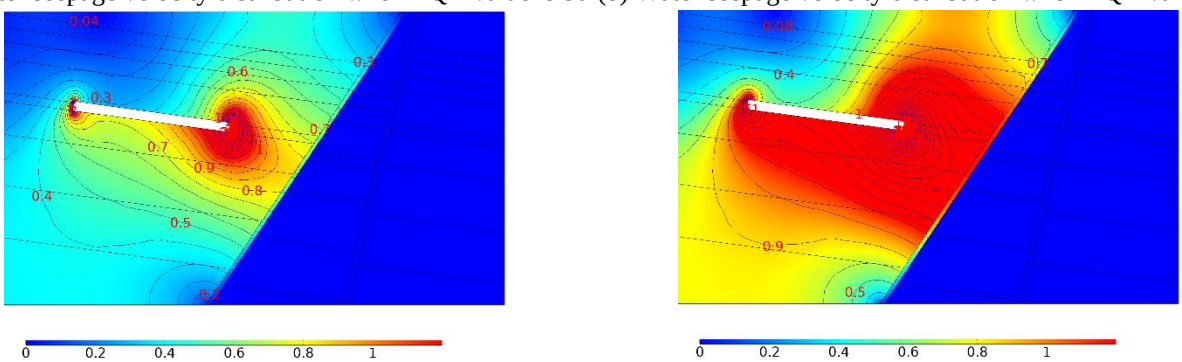

(c) Water seepage velocity distribution when RQD value is 30 (d) Water seepage velocity distribution when RQD value is 10

Fig. 13 Seepage velocity distribution in mining floor with different RQD values

Fig. 12 shows the distribution characteristics of stope pore water pressure when RQD value of floor rock mass is 80, 60, 30 and 10, respectively. Fig. 13 shows the seepage velocity distribution characteristics of pore water when RQD value of floor rock mass is 80, 60, 30 and 10, respectively. As the RQD value gradually decreases, the seepage velocity gradually increases. It can be seen from the figure that the stress distribution state of the original rock is destroyed by the influence of mining, and the permeability of the rock mass changes. This affects the flow path and flow state of the aquifer and creates a pressure relief zone near the working face.

With the decrease of rock mass RQD value, the frequency of fracture surface in rock mass increases, the rock mass is more broken, and the water inflow in goaf increases. Therefore, the pore water pressure in stope also decreases. The change process is the same as that of hydraulic pressure monitoring in actual mining. With the increase of the overall RQD index of mine rock mass, the mine water inflow increases rapidly. This indicates that the more broken rock mass, the greater the daily mine water inflow value. When RQD value tends to 100, mine inflow tends to 0. This indicates that when the rock mass is not damaged, the mine water inflow is small.

The data of water gushing in the first mining face of the mine are analyzed, and the statistical results are shown in Fig. 14. With the development of mining, the mine water inflow gradually increases, and the maximum water inflow of working face is basically kept at 600 m^3/h. Table 2 shows the statistical results of rock mass RQD quality index in the treatment process of Ordovician limestone water. As can be seen from the table, the average RQD of limestone rock

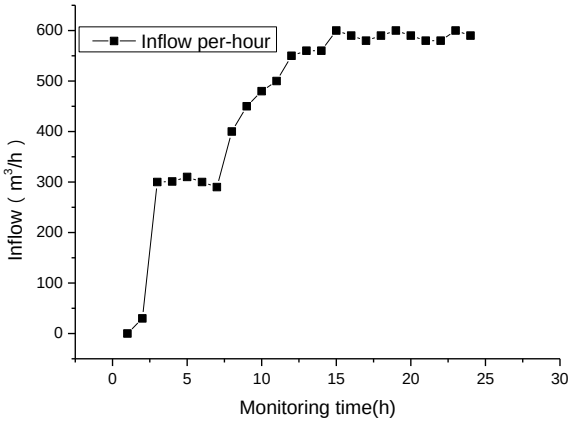

Fig. 14 Statistical duration curve of water inflow on 201 first mining face of a mine in in a feicheng

Table 2 RQD statistics of drilling hole on the 201 first mining face of lower coal group in a feicheng mine

Olympic ash grouting hole number	RQD		
	Shale rock group	Sandstone rock group	Limestone rock group
Hole 1	0.45	0.66	0.72
Hole 2	0.44	0.55	0.88
Hole 3	0.38	0.57	0.82
Hole 4	0.40	0.62	0.85
Hole 5	0.46	0.63	0.93
Hole 6	0.35	0.56	0.80
Hole 7	0.38	0.44	0.83
Hole 8	0.44	0.56	0.79
Hole 9	0.47	0.65	0.82
Hole 10	0.33	0.63	0.90

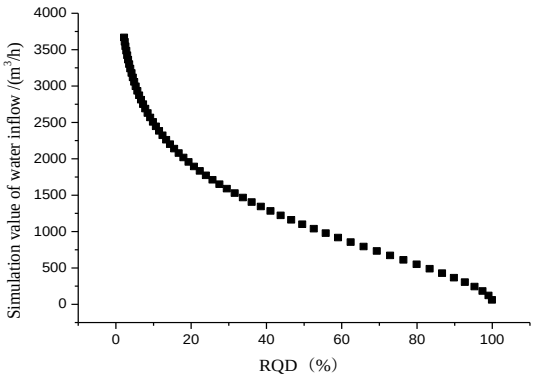

Fig. 15 changes of RQD values of different rock masses in water inrush and daily water inflow

mass is about 80%. The simulated inflow of working face is about 550 m^3/h (Fig. 15). This is basically consistent with the monitoring results.

In the actual exploration process, the distribution characteristics of fractures in boreholes are analyzed. It can be used to calculate water inflow by the method and procedure presented in this paper. In the prediction of mine water inflow, the calculation domain can be determined by grasping the law of crack development and the dimension of exploiting space. This generates a two-dimensional fracture network model of the open space section. The numerical model can be loaded by detecting the boundary water head value of the model, and the expected water inflow of blocks represented by different RQD values can be calculated. The water inflow of the mine was determined by calculating RQD value, and the parameters of fracture connectivity and water conductivity were corrected by hydrogeological test. This is used for inflow analysis calculations to save time and investment. Of course, the calculation method of water inflow in this paper must satisfy that there cannot be centralized seepage channels. The rock mass as a whole is micro-fractured and can be described by RQD, so only RQD can exist the correlation between RQD and water pressure and seepage parameters. As shown in Fig. 16, confined water affected by faults is mainly affected by fault water diversion, and changes in rock mass RQD value have little influence on mine water intrusion. At this point, the calculation should be based on fault inflow, which is consistent with the actual situation.

4. Research on grouting quantity prediction based on RQD index

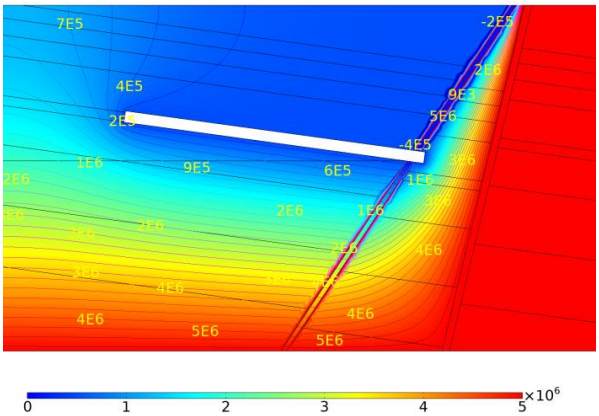

(a) Stope water pressure distribution when RQD value is 80 under the influence of faults

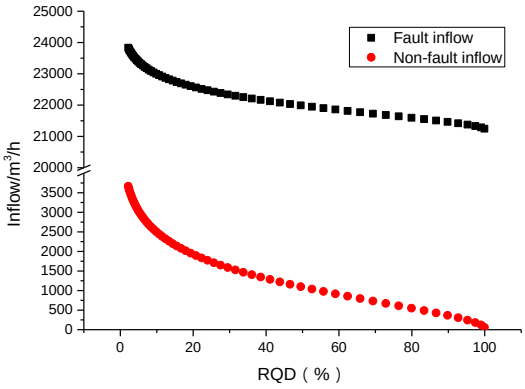

(b) Changes of water inrush and daily water inflow with RQD values of different rock masses

Fig. 16 Distribution characteristics of pore water pressure in stope under the influence of faults

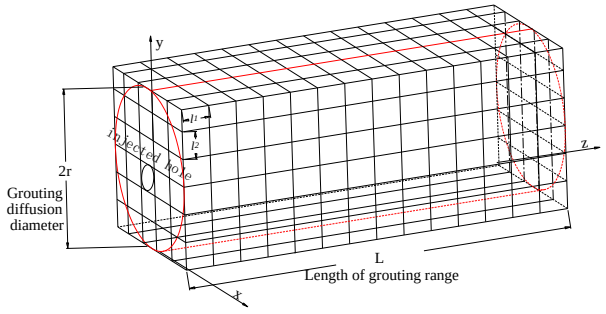

(a) Sketch of borehole and fissure grouting body

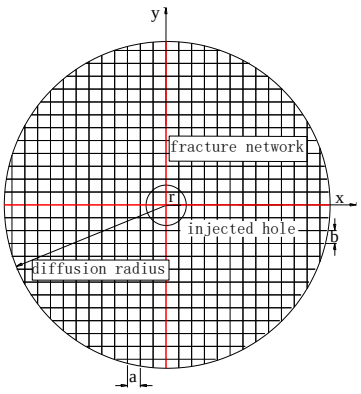

(b) Sketch diagram of fracture network and diffusion radius of grouting section

Fig. 17 Schematic diagram of grouting in borehole and fissure

4.1 Simplified methods of different fracture direction vectors

RQD has magnitude and direction. However, the RQD obtained in vertical drilling can be applied to other calculation directions by transformation. This can approximately obtain the upper and lower limits of the total permeability coefficient and be applied to the prediction and forecast of mine water inflow (Yin *et al.* 2011, Cai *et al.* 2020, He *et al.* 2019). Based on the isotropy hypothesis of rock mass, the total volume within the diffusion range of grouting remains unchanged for the convenience of quantitative research. The mean width b and the connectivity coefficient η of the crack are introduced. It modifies the permeability calculation formula (LEUNG *et al.* 2012, Zhang *et al.* 2020), and the schematic diagram of borehole and fissure grouting is shown in Fig. 16. Based on the above assumptions, this paper establishes the relationship between the number of fractures and the amount of grouting in fractured rock mass.

4.2 Grouting quantity forecast

When the fracture direction is horizontal and vertical, the slurry diffusion radius is set as R, and the grouting length is set as L. The average width of the fissure monitored by probing boreholes is T. The cyclic footage is l_1. The frequency of cracks in the circulation is λ. The coefficient of fracture connectivity is η which is shown in Fig. 17.

According to the geometrical relation, it is assumed that the grouting diffusion range is cylindrical. Then the overall volume of fractures in the horizontal direction is

$$T_1 = \pi r^2 t_1 \frac{L}{l_1} \lambda_1 \tag{12}$$

The vertical drilling direction is assumed to be a and B, respectively. According to geometric relations, the total volume of fractures in vertical drilling direction is approximately

$$T_2 = \frac{\pi r^2}{a \cdot b} a t_2 \frac{L}{l_2} \lambda_2 + \frac{\pi r^2}{a \cdot b} a t_3 \frac{L}{l_3} \lambda_3 \tag{13}$$

Where

$$a = \frac{l}{\lambda_2}, b = \frac{l}{\lambda_3}$$

$$Q = (T_1 + T_2)\eta \tag{14}$$

RQD can be used to calculate the number of cracks and obtain the permeability coefficient parameter represented by *RQD*.

The above special cases with horizontal and vertical fractures were analyzed and the calculation method of grouting quantity was obtained. When the dominant water conduction direction of the fracture is at a certain Angle with the horizontal and vertical directions, the calculation can be carried out by referring to the solution method of the permeability tensor of the fractured rock mass. At this point, the formula is modified as:

Overall volume of fractures in the horizontal direction

$$T_{1\alpha} = \pi r^2 t_1 \frac{L}{l_1} \lambda_1 / \cos\alpha \tag{15}$$

Table 3 Field grouting statistics and calculation results of average crack width

Hole No.	Length *L/m*	Final pressure (MPa)	Average gap width/m×10^{-5}	Total plasma quantity *Q/t*
D3-0	766.98	10.5	3.59	1020
D3-1	361.23	12.0	8.81	570
D3-2	501.79	12.5	1.15	1415
D3-3	594.46	13.0	4.57	785
D3-4	636.02	13.0	3.77	740
D3-7	357.66	13.0	5.52	350
D3-5	696	13.0	7.14	1675
D3-6	761.12	13.0	1.24	3460
D10-0	488.45	9.5	2.92	3405
D10-6	586.04	13.0	1.91	3190
D10-4	485.74	10.5	1.08	12450
D10-5	525.52	7.5	7.85	10570
D10-3	539.67	7.5	5.64	7995
D10-2	462.29	7.5	5.33	5575

The total volume of fractures in the vertical direction

$$T_{2\beta\gamma} = \frac{\pi r^2}{a \cdot b} a t_2 \frac{L}{l_2} \lambda_2 / \cos\beta + \frac{\pi r^2}{a \cdot b} a t_3 \frac{L}{l_3} \lambda_3 / \cos\gamma \tag{16}$$

Where, α, β and γ are fracture strike, dip and dip Angle respectively. When the fracture permeability tensor obtained by cyclic footage varies greatly, more accurate data can be obtained by grouping calculation.

4.3 Prediction results and analysis

Taking the grouting example of D3 and D10 holes in a coal mine for verification, the *RQD* of the grouting section is 60, and the return footage is 2 m. According to the formula 5, the frequency of fractures is 14, that is, there are 14 fractures within 2 meters of cyclic penetration. If the grouting radius is 40 meters, the average crack width can be calculated according to the formula, as shown in Table 3. In practice, it is only necessary to measure the average fissure opening of boreholes. It can be applied to the prediction of grouting quantity. The difference between the calculated grouting amount and the on-site grouting amount is less than 10%, indicating that the theoretical calculation method of grouting amount is reasonable to a certain extent.

5. Conclusions

1) Based on the characteristics of rock mass quality index, seepage experiments with different frequency of longitudinal fractures were carried out. A numerical model of orthogonal fracture network was established to obtain the exponential relationship between fracture frequency and seepage velocity.

(2) The basic principle of Monte-Carlo method is applied. The random crack generation program was written by MATLAB and imported into the interface with Comsol Multiphysics to generate the numerical calculation model of fractured rock mass. On this basis, the simulation research of different random fracture

frequency is carried out. The study shows that the relationship between fracture frequency and pressure conforms to exponential function. The RQD index combined with fracture frequency can be used to predict water inflow.

(3) Based on the case of on-site grouting water control project, rock mass quality index is used to estimate the amount of mine grouting. A new grouting quantity prediction method considering fracture opening and fracture connectivity is proposed. In practical engineering, the average crack opening of borehole is measured. It can be used to predict the amount of grouting. The research results are great significant to the prediction of mine water inflow and safety evaluation of water inrush disaster management.

Expectation

(1) Due to the relatively small amount of data from in-situ drilling water injection test, this paper uses the width of borehole core fissure to calculate the grouting amount. In the later work, the relationship between crack width and grouting quantity should be further verified.

(2) Limited to laboratory conditions, this paper only carried out an experimental study on orthogonal fractures. This verifies the rationality of the numerical simulation. In the follow-up work, experiments on oblique fractures and fractures of different frequencies will be carried out. Compared with numerical simulation, it provides further validation for numerical simulation.

Acknowledgments

This study was funded by National Natural Science Foundation of China (Grant Nos. 52104203, 51974172, 51904168). Shandong Province Natural Science Foundation Project (ZR2020QE128, ZR2020ME102, ZR2021ME138), Scientific Research Foundation of Key Laboratory of Mining Disaster Prevention and Control (MDPC202012), National Key R&D Program of China (2018YFC0604705), SDUST Research Fund (grant 2018TDJH102), National Natural Science Foundation of China (Grant nos. 51574159, 52074251, 51974172, 51974173, 92058211 and 51804179), Central Universities (No. 842012003), and 111 project (No. B20048). Central Universities (No. 842012003), and 111 project (No. B20048).

References

Annaidh, A.N., Destrade, M., Gilchrist, M.D. and Murphy, J.G. (2013), "Deficiencies in numerical models of anisotropic nonlinearly elastic materials", *Biomecha. Model. Mechanobiology*, **12**(4), 781-791. https://doi.org/10.1007/s10237-012-0442-3.

Cai, X., Cheng, C., Zhao, Y., Zhou, Z. and Wang, S. (2022), "The role of water content in rate dependence of tensile strength of a fine-grained sandstone", *Arch. Civil Mech. Eng.*, **22**(1), 1-16. https://doi.org/10.1007/s43452-022-00379-8.

Cai, X., Zhou, Z., Zang, H. and Song, Z. (2020), "Water saturation effects on dynamic behavior and microstructure damage of sandstone: Phenomena and mechanisms", *Eng. Geology*, **276**, 105760. https://doi.org/10.1016/j.enggeo.2020.105760.

Chen, J., Zhao, J., Zhang, S., Zhang, Y., Yang, F. and Li, M. (2020), "An experimental and analytical research on the evolution of mining cracks in deep floor rock mass", *Pure Appl. Geophys.*, **177**(11), 5325-5348. https://doi.org/10.1007/s00024-020-02550-9.

Chen, J.P., Fan, J.H. and Liu, D. (2005), "A review and prospect on the application and research of RQD", *Rock Soil Mech.*, **26**(S2), 249-252.

Chen, M.Z., Liu, S.C. and Yang, G.Y. (2009), "The development of mining water in flow predict method", *Chin. J. Eng. Geophys.*, **6**(1), 68-72.

Cheng, X.G., Qiao, W., Lu, L., Jiang, C.W. and Lei, N. (2020), "Model of mining-induced fracture stress-seepage coupling in coalseam over-burden and prediction of mine inflow", *J. China Coal Soc.*, **45**(08), 2890-2900.

Deere, D.U. (1963), "Technical description of rock cores for engineering purposes", *Rock Mech. Eng. Geol.*, **1**(1), 18-22.

Du, M.M., Deng, Y.E. and Xu, M. (2009), "Review of methodology for prediction of water yield of mine", *Acta Geologica Sinica*, **29**(1), 70-73.

Euser, B., Rougier, E., Lei, Z., Knight, E.E., Frash, L.P., Carey, J. W., ... & Munjiza, A. (2019), "Simulation of fracture coalescence in granite via the combined finite-discrete element method", *Rock Mech. Rock Eng.*, **52**(9), 3213-3227. https://doi.org/10.1007/s00603-019-01773-0.

Ghyasvand, S., Fahimifar, A. and Nejad, F.M. (2022), "On the optimum design of reinforcement systems for old masonry railway tunnels", *Geomech. Eng.*, **28**(2), 145-155. https://doi.org/10.12989/gae.2022.28.2.145.

Guo, W.J., Zhao, J.H., Yin, L.M. and Kong, D.Z. (2017), "Simulating research on pressure distribution of floor pore water based on fluid-solid coupling", *Arab. J. Geosci.*, **10**(1), 1-14. https://doi.org/10.1007/s12517-016-2770-6.

He, C., Yao, C., Yang, J. *et al.* (2019), "A 3D model for flow in fractured rock mass based on the equivalent discrete fracture network", *Chin. J. Rock Mech. Eng.*, **38**(S1), 2748-275.

Hudson, J.A. and Harrison, J.P. (2000), *Engineering Rock Mechanics: An Introduction To The Principles*, Elsevier.

Ibishi, G., Genis, M. and Yavuz, M. (2022), "Post-pillars design for safe exploitation at Trepca hard rock mine "(Kosovo) based on numerical modeling", *Geomech. Eng.*, **28**(5), 463-475. https://doi.org/10.12989/gae.2022.28.5.463.

Jha, B. and Juanes, R. (2014), "Coupled multiphase flow and poromechanics: A computational model of pore pressure effects on fault slip and earthquake triggering", *Water Resour. Res.*, **50**(5), 3776-3808. https://doi.org/10.1002/2013WR015175.

Karatela, E. and Taheri, A. (2018), "Three-dimensional hydro-mechanical model of borehole in fractured rock mass using discrete element method", *J. Nat. Gas Sci. Eng.*, **53**, 263-275. https://doi.org/10.1016/j.jngse.2018.02.032.

Khorasani, E., Amini, M., Hossaini, M.F. and Medley, E. (2019), "Evaluating the effects of the inclinations of rock blocks on the stability of bimrock slopes", *Geomech. Eng.*, **17**(3), 281-287. https://doi.org/10.12989/gae.2019.17.3.281.

Kim, E., Garcia, A. and Changani, H. (2018), "Fragmentation and energy absorption characteristics of Red, Berea and Buff sandstones based on different loading rates and water contents", *Geomech. Eng.*, **4**(2), 151-159. https://doi.org/10.12989/gae.2018.4.2.151.

Komurlu, E., Kesimal, A. and Demir, S. (2016), "Experimental and numerical analyses on determination of indirect (splitting)

tensile strength of cemented paste backfill materials under different loading apparatus", *Geomech. Eng*., **10**(6), 775-791. https://doi.org/10.12989/gae.2016.10.6.775.

Lawal, A.I., Kwon, S., Aladejare, A.E. and Oniyide, G.O. (2022), "Prediction of the static and dynamic mechanical properties of sedimentary rock using soft computing methods", *Geomech. Eng*., **28**(3), 313-324. https://doi.org/10.12989/gae.2022.28.3.313.

Leung, C.T. and Zimmerman, R.W. (2012), "Estimating the hydraulic conductivity of two-dimensional fracture networks using network geometric properties", *Trans. Porous Media*, **93**(3), 777-797. https://doi.org/10.1007/s11242-012-9982-3.

Li, L.P., Chen, D.Y., Li, S.C., Shi, S.S., Zhang, M.G. and Liu, H.L. (2017), "Numerical analysis and fluid-solid coupling model test of filling-type fracture water inrush and mud gush", *Geomech. Eng*., **13**(6), 1011-1025. https://doi.org/10.12989/gae.2017.13.6.1011.

Lin, B. (2010), "Research of water yield prediction of mine about a uranium deposit in north east of guangdong province", *Resour. Environ. Eng.*, **24**(3), 293-296.

Liu, Y.Z., Sheng, J.L., Ge, X.R. and Wang, S.L. (2007), "Evaluation of rock mass quality based on fractal dimension of rock mass discontinuity distribution", *Yantu Lixue(Rock Soil Mech.)*, **28**(5), 971-975.

Lu, Z.G., Yao, J., Wang, D.S. and Li, L. (2010), "Experimental study on fluid flow characteristic in orthogonal fracture network", *J. China Coal Soc.*, **35**(04), 555-558.

Lv, H.Y, Tang, Y.S., Zhang, L.F., Cheng, Z.B. and Zhang, Y.N. (2019), "Analysis for mechanical characteristics and failure models of coal specimens with non-penetrating single crack", *Geomech. Eng*., **17**(4), 355-365. https://doi.org/10.12989/gae.2019.17.4.355.

Mahmoodzadeh, A., Mohammadi, M., Abdulhamid, S.N., Ali, H.F.H., Ibrahim, H.H. and Rashidi, S. (2022), "Forecasting tunnel path geology using Gaussian process regression", *Geomech. Eng*., **28**(4), 359-374, https://doi.org/10.12989/gae.2022.28.4.359.

Maruvanchery, V. and Kim, E. (2019), "Effects of water on rock fracture properties: Studies of mode I fracture toughness, crack propagation velocity, and consumed energy in calcite-cemented sandstone", *Geomech. Eng.*, **17**(1), 57-67. https://doi.org/10.12989/gae.2019.17.1.057.

Morrison, K.G., Reynolds, J.K. and Wright, A. (2019), "Subsidence fracturing of stream channel from longwall coal mining causing upwelling saline groundwater and metal-enriched contamination of surface waterway", *Water Air Soil Pollut*., **230**, 1-13. https://doi.org/10.1007/s11270-019- 4082-4.

Mottahedi, A. and Ataei, M. (2019), "Fuzzy fault tree analysis for coal burst occurrence probability in underground coal mining", *Tunnel. Underg. Space Technol.*, **83**, 165-174. https://doi.org/10.1016/j.tust.2018.09.029.

Munoz, H., Taheri, A. and Chanda, E.K. (2016), "Pre-peak and post-peak rock strain characteristics during uniaxial compression by 3D digital image correlation", *Rock Mech. Rock Eng.*, **49**(7), 2541-2554. https://doi.org/10.1007/s00603-016-0935-y.

Priest, S.D. and Hudson, J.A. (1976), "Discontinuity spacings in rock", *Int. J. Rock Mech. Min Sci. Geomech. Abstr.*, **13**(5), 135-148. https://doi.org/10.1016/0148-9062(76)90818-4.

Samanta, M., Punetha, P. and Sharma, M. (2018), "Effect of roughness on interface shear behavior of sand with steel and concrete surface", *Geomech. Eng*., **14**(4), 387-398. https://doi.org/10.12989/gae.2018.14.4.387.

Sweetenham, M.G., Maxwell, R.M. and Santi, P.M. (2017), "Assessing the timing and magnitude of precipitation-induced seepage into tunnels bored through fractured rock", *Tunnel. Underg. Space Technol.*, **65**, 62-75. https://doi.org/10.1016/j.tust.2017.02.003.

Vaziri, M.R., Tavakoli, H. and Bahaaddini, M. (2022), "2D numerical study of the mechanical behaviour of non-persistent jointed rock masses under uniaxial and biaxial compression tests", *Geomech. Eng*., **28**(2), 117-133. https://doi.org/10.12989/gae.2022.28.2.117.

Wan, D., Hu, C. and Xing, W. (2018), "Application of discrete fracture network model to mine water inflow prediction", *J. Hebei GEO Univ.*, **41**(01), 65-69.

Wan, L., Wang, J., Zeng, Q., Ma, D., Yu, X. and Meng, Z. (2022), "Vibration response analysis of the tail beam of hydraulic support impacted by coal gangue particles with different shapes", *ACS omega*, **7**(4), 3656-3670., https://doi.org/10.1021/acsomega.1c06279.

Wang, E.Z., Sun, Y., Huang, Y.Z. and Wang, H.M. (2002), "3-D seepage flow model for discrete fracture network and verification experiment", *J. Hydraul. Eng.*, **5**, 37-40.

Wang, G. (2006), "Threedimensional simulation of rock joints and permeability tensor analysis", *Wuhan Institute of Rock and Soil Mechanics*, Chinese Academy of Sciences, Wuhan.

Wei, X. and Yang, C.H. (2015), "A method of geometric parameter determination of drilling rock fractures", *Chin. J. Rock Mech. Eng.*, **34**(9), 1758-1766.

Xiao-wei, J., Li, W.A.N., Xu-sheng, W.A.N.G., Xiong, W. and Hui-hong, C. (2009), "Estimation of depth-dependent hydraulic conductivity and deformation modulus using RQD", *Rock Soil Mech.*, **30**(10), 3163-3167.

Xue, Y.C., Sun, W.B. and Wu, Q.S. (2020), "The influence of magmatic rock thickness on fracture and instability law of mining surrounding rock", *Geomech. Eng*., **20**(6), 547-556. https://doi.org/10.12989/gae.2020.20.6.547.

Yamada, Y., Yoshimura, N. and Sakurai, T. (1968), "Plastic stress-strain matrix and its application for the solution of elastic-plastic problems by finite element method", *Int. J. Mech. Sci.*, **10**, 343-354. https://doi.org/10.1016/0020-7403(68)90001-5.

Yang, Y., Han, B., Xie, K. *et al.* (1995), "To Forecast the water yield of coal mine applying the mine series interrelated model with multivariation", *Coal Geol. Explor.*, **23**(6), 38-42.

Yanqing, W. (1998), "Determination methods of hydraulic parameters of rock mass (7)", *Hydrogeol. Eng. Geol.*, **25**(2), 42-48.

Yin, D., Wang, W. and Chen, S. (2011), "Block element method for seepage-stress coupling in random fractured rock", *Rock Soil Mech.*, **32**(09), 2861-2866.

Zeng, Y., Lian, H., Du, X., Tan, X. and Liu, D. (2022), "An analog model study on water–sand mixture inrush mechanisms during the mining of shallow coal seams", *Mine Water Environ.*, 1-9.

Zeng, Y., Pang, Z., Wu, Q., Hua, Z., Lv, Y., Wang, L., ... & Liu, S. (2022), "Study of water-controlled and environmentally friendly coal mining models in an ecologically fragile area of Northwest China", *Mine Water Environ.*, 1-15. https://doi.org/10.1007/s10230-022-00871-w.

Zhang, J., Sheng, J., Huang, T. *et al.* (2020), "Research on permeability and connectivity of 2D fracture network", *Indus. Miner. Proc.*, **49**(07), 6-10.

Zhang, Y.H., Zhou, H.W. and Xie, H.P. (2005), "Improved cubic covering method for fractal dimensions of a fracture surface of rock", *Chin. J. Rock Mech. Eng.*, **24**(17), 3192-3196.

Zhao, J., Chen, J., Zhang, X., Jiang, N. and Zhang, Y. (2020a), "Distribution characteristics of floor pore water pressure based on similarity simulation experiments", *Bull. Eng. Geol. Environ.*, **79**(9), 4805-4816. https://doi.org/10.1007/s10064-020-01835-6

Zhao, J., Juntao, C., Huilin, X., Zhao, Z. and Xinguo, Z. (2022), "Dynamic mechanical response and movement evolution characteristics of fault systems in the coal mining process", *Pure Appl. Geophys.*, **179**, 233-246. https://doi.org/10.1007/s00024-021-02905-w.

Zhao, J., Zhang, X., Ning, J., Yin, L. and Guo, W. (2020b), "Porosity characteristics of fault floor under fluid-solid

coupling", *Bull. Eng. Geol. Environ.*, **79**(5), 2529-2541. https://doi.org/10.1007/s10064-019-01701-0.

Zhao, J.H., Yin, L.M. and Guo, W.J. (2018), "Stress-seepage coupling of cataclastic rock masses based on digital image technologies", *Rock Mech. Rock Eng.*, **51**(8), 2355-2372. https://doi.org/10.1007/s00603-018-1474-5.

Zhou, C., Ye, Z., He, J. *et al.* (1998), "Probability models and stochastic simulation of rock joints opening", *Chin. J. Rock Mech. Eng.*, **17**(3), 267-272.

Zhou, F., Sun, W.B., Shao, J.L., Kong, L.J. and Geng, X.Y. (2020), "Experimental study on nano silica modified cement base grouting reinforcement materials", *Geomech. Eng.*, **20**(1), 67-73. https://doi.org/10.12989/gae.2020.20.1.067.

Zhou, Z. and Wang, J. (2004), *Fissure Medium Hydrodynamics*. Water and Power Press, Beijing.

Zhou, Z., Cai, X., Li, X., Cao, W. and Du, X. (2020), "Dynamic response and energy evolution of sandstone under coupled static-dynamic compression: insights from experimental study into deep rock engineering applications", *Rock Mech. Rock Eng.*, **53**, 1305-1331. https://doi.org/10.1007/s00603-019-01980-9.

IC